



## Experimental studies on thermal spray-coated horizontal tubes for falling film evaporation in multi-effect desalination system

Raju Abraham<sup>a,\*</sup>, A. Mani<sup>b</sup>

<sup>a</sup>National Institute of Ocean Technology, Velachery-Tambram Road, Chennai 600 100, India, email: [abraham@niot.res.in](mailto:abraham@niot.res.in)

<sup>b</sup>Department of Mechanical Engineering, Indian Institute of Technology Madras, Chennai 600 036, India, email: [mania@iitm.ac.in](mailto:mania@iitm.ac.in)

Received 3 October 2013; Accepted 3 June 2014

---

### ABSTRACT

Multi-effect distillation is an important principle in desalination technology, in which the thin film evaporation of sea water takes place at the outer surface of bundle of tubes, normally arranged in horizontal. Heat of condensation inside the tube is transferred to the falling water film by conduction, thereafter convective evaporation of film takes place. Heat transfer on the outside is unpredictable due to the uncertainty in nature of film, film thickness, film dryout, etc. and film coefficient is considerably less compared to inside. Thermal spray coating on metallic surface with molten metal particles create porous surface which enhances heat transfer due to higher turbulence and nucleation sites, if sufficient temperature difference available. This paper discusses the experimental studies carried out on a  $3 \times 5$  bundle of 25.4 mm  $\varnothing$  Al horizontal tubes with thermal spray coating of aluminum. Influences on temperature profile, heat transfer coefficient, mass evaporation, etc. are studied. A comparison of sea water and fresh water is carried out for the performance of the system. The experimental setup is established at IIT Madras, Chennai, India.

*Keywords:* Falling film evaporation; Film heat transfer coefficient; Heat transfer enhancement; Mass evaporation

---

### 1. Introduction

Heat transfer studies on falling film evaporation are gaining momentum due to the applications in desalination and process industries. There were several theoretical and experimental studies in the past on film modeling, effects of various operating parameters, tube configuration, heat transfer enhancement techniques, etc. There are few publications on the computational studies on the film flow around the horizontal circular tube. Heat transfer enhancement techniques such as structured surfaces or porous

metallic coatings, grooved surfaces and extended surfaces such as fins are studied in the past for various applications in aerospace, nuclear technology, refrigeration, power generation, chemical industries, etc. Metallic spray coating on heat transfer surface has been widely reported in recent years for heat transfer enhancement. This paper discusses the experimental studies on falling film evaporation on bare tubes and thermal spray-coated tubes with heat transfer enhancement.

One of the earliest experimental studies on falling film evaporation was conducted by Fletcher et al. [1] on horizontal Cu–Ni alloy tube for evaporation of sea water. An increase in heat transfer coefficient is

---

\*Corresponding author.

observed with respect to feed rate, heat flux, and saturation temperature. Parken et al. [2] conducted experimental studies on electrically heated brass tubes of 25.4 and 50.8 mm diameter for measuring film coefficients under boiling and convective evaporation conditions for transient flow over the plain tube. It was observed that local film coefficient increases with feed rate, inlet water temperature for non-boiling conditions, but is independent of heat flux through the wall. For boiling conditions, heat transfer coefficient is increased with feed water temperature and wall heat flux. It was also observed large fluctuations in film coefficient under local boiling conditions. Studies by Tewari et al. [3] on 19 mm  $\varnothing$ , SS 316 tube, heated with dry saturated steam with a wall super heat of 5–16 K showed the presence of nucleate boiling under sub-atmospheric pressure conditions. The influences of feed rate, saturation pressure, etc. were studied. Experimental studies of Hu and Jacobi [4] focused on modes of falling film flow such as drop, jet, and sheet modes with three different working fluids. A map for predicting flow pattern was developed based on Reynolds number ( $Re$ ) and Galileo number ( $Ga$ ). Influence of fluid properties, flow rate, tube diameter, tube spacing etc. were studied. Yang and Shen [5] reported the experimental studies on Al-brass tube of 14 mm  $\varnothing$  under uniform heat flux with electric heating. The influence of non-condensable gas was found significant on heat transfer coefficient. Tests were carried out with sea water and fresh water. Experimental studies with varying tube diameters (20–32 mm), inter-tube spacing (10–40 mm), and falling film Reynolds number (150–800) were carried out by Hou et al. [6]. Chyu and Bergles [7] presented experimental data on falling film evaporation with structured surfaces. Alam et al. [8] carried out studies on heat transfer enhancement by copper coating of various thicknesses on a 32 mm outside diameter mild steel tube for pool-boiling conditions. Lakhera et al. [9] studied the effect of porous thermal spray coating of stainless steel 316 on plain AISI 304 tube having 19.05 mm outer diameter and 130 mm length under flow boiling conditions for distillate water at atmospheric pressure. Li et al. [10] conducted experimental studies on a bundle of horizontal tubes for falling film convective evaporation using enhanced surfaces such as Turbo-CAB, Korodense, etc. Most of these studies with thermal spray coating are applied to pool boiling. Computational studies on falling evaporation with heat transfer enhancement were presented by Abraham and Mani [11]. Overall review on falling film evaporation has been given by Ribatski and Jacobi [12].

## 2. Heat and mass transfer in falling film evaporation

In falling film evaporation for desalination applications, the low pressure vapor is condensed inside the tube exchanging heat to the thin film outside. Latent heat of condensation is transferred through the film resulting in the convective evaporation of water at liquid–vapor interface. Local temperature difference between the tube wall surface and vapor is normally less than 5°C and hence nucleate boiling doesn't take place. The gravitational flow of film around a tube is divided into four regions as described by Chyu and Bergles [13] and shown in Fig. 1. Feed water is sprayed over the single tube surface at a rate of  $2\Gamma$  (kg/m/s) where  $\Gamma$  is the liquid mass flow rate per side per unit length of the tube. The tube surface temperature is maintained at  $T_w$ °C. The vapor region around the tube is maintained at vacuum condition corresponding to the saturation temperature ( $T_s$ ) of feed water. Flow mode between two vertical tubes depends on the falling film Reynolds number and is classified as drop mode, jet mode, and sheet mode as discussed in the studies of Hu and Jacobi. Film Reynolds number, the influencing parameter for heat transfer coefficient, is defined as the ratio of inertia force to viscous force in the falling film. Experimental studies show that the transition from droplet mode to the jet mode occurs at  $Re=150$ – $200$  and the transition from jet mode to sheet mode occurs at  $Re=315$ – $600$  for water.

Heat transferred across the tube wall is utilized for the evaporation of the fluid and heating of the downstream flow and can be related as:

$$q_w = m_f h_{fg} + (m_i - m_f) C_{pl} (T_{fo} - T_{fi}) \quad (1)$$

Heat conducted along the thin film is related to the outside film coefficient in terms of temperature difference across the wall and saturation temperature of vapor.

$$q_f = k \frac{dT}{dr} = h_o (T_w - T_s) \quad (2)$$

Mass flow of liquid into the tube is given as

$$m_i = 2L\Gamma \quad (3)$$

Total mass of liquid evaporated from the film is related as

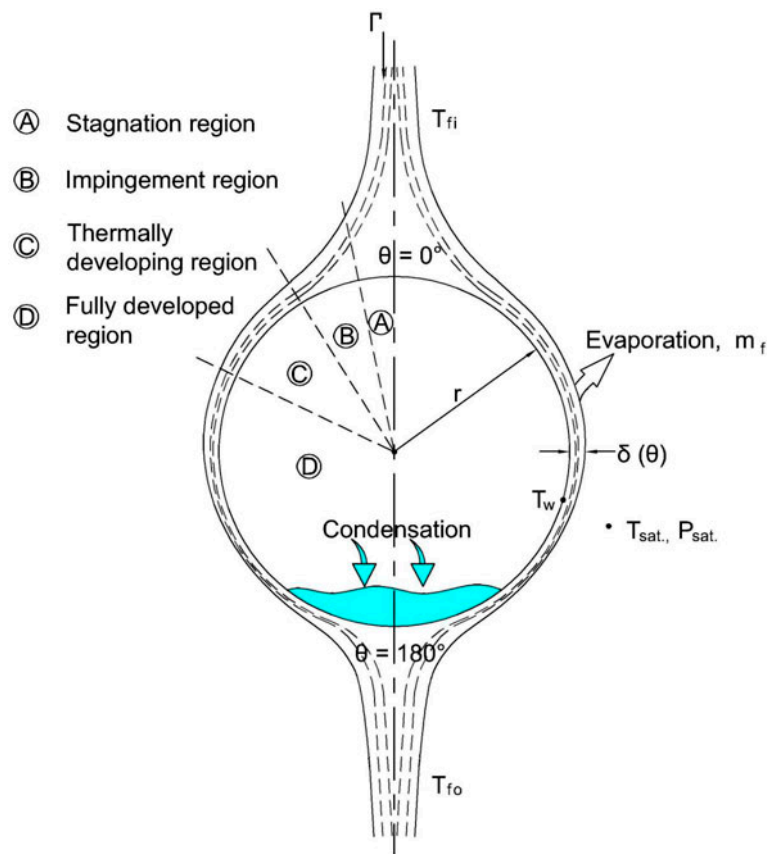


Fig. 1. Film-flow regions around a horizontal tube.

$$m_e = \frac{h_o A (T_w - T_s)}{C_{pl} (T_s - T_{fi}) + h_{fg}} \quad (4)$$

Thus the feed flow rate, feed water temperature, fluid properties, tube configuration, etc. play an important role in heat and mass transfer of falling film evaporation systems. Porous metallic coating on the tube surface enhances the turbulence level, reduction in film thickness, possibility of nucleation, etc. and improves the overall performance of the system.

### 3. Experimental setup

An extensive experimental setup on horizontal tube falling film for studying the effect of feed flow, feed water temperature, and tube configuration, etc. was designed as per the schematic shown in Fig. 2. The experimental system was fabricated as shown in Fig. 3 at Refrigeration and Air-conditioning laboratory at Indian Institute of Technology, Madras (IITM) in Chennai. The detailed specification of the experimental system is given in Table 1. It consists of an

evaporator with 0.5 m  $\varnothing \times 1.5$  m long shell with 15 numbers of Aluminum tubes of 25.4 mm OD  $\times$  1.4 m long. The tubes can be easily removed and re-fitted as it is fixed with special grommets. Plain and thermal spray-coated tubes were tested. Tube sheet also can be interchanged to test the different configurations of tubes. There is a 3  $\times$  5 matrix for the tube bundle arrangement. The top two rows are used as dummy tubes for flow stabilization. The bottom three rows are inserted with electric heaters (Table 2). Falling water film over the evaporator tubes is heated using electrical heaters inside the tube. The heater is fixed with temperature controller based on the tube wall temperature measured. Tube wall temperatures are measured using thermocouples fixed on the tube surface as shown in Fig. 4(a). Digital voltmeter and ammeter were used to measure the power input. Polypropylene tubes with tiny opening at the bottom are fixed on the top of Aluminum tubes for spraying water over the tube bundle as in Fig. 4(b). Two view glasses of 200 mm  $\varnothing$  were placed on each side of the evaporator for clear inside view and falling film visualization.

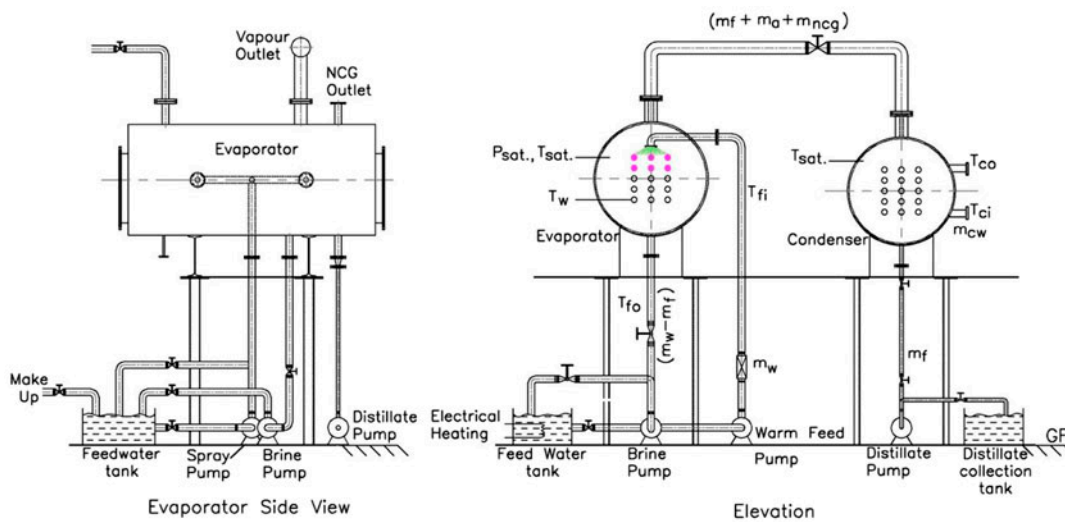


Fig. 2. Schematic diagram of the experimental setup.

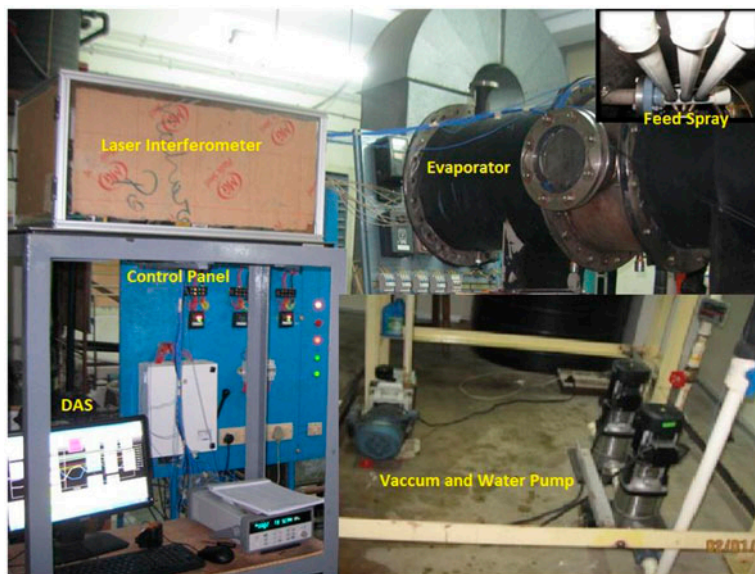


Fig. 3. Experimental setup for falling film studies with water.

Condenser is of the similar dimensions as of evaporator with 18 tubes. The vapor generated is flowing to the condenser, where condensation takes place due to the cooling water circulated inside the tubes. Vacuum is maintained inside the system with a vacuum pump connected to the condenser. Centrifugal pumps are used for the circulation of water in the evaporator and condenser. The complete system is instrumented to measure the heat transfer characteristics. There is a hot water generating system with temperature regulation up to 0.1°C accuracy. The

feed water for falling film evaporation can be heated to a maximum of 80°C. Similarly, a chilling system is used to supply required cold water to the condenser. Electric cartridge heaters each of about 3 kW capacities were used to maintain a constant wall temperature on the tube surface. The evaporator, condenser, and piping were insulated to prevent heat interaction with atmosphere. Complete experimental system is positioned at about 1.4 m above ground level for creating positive suction head to the pumps.

Table 1  
Specification of the experimental setup

Parameters		
1.	Shell diameter	500 mm
2.	Shell material	SS 316 L
3.	Shell thickness	6 mm
4.	Tube diameter and thickness	25.4 mm × 1 mm
5.	Effective length of tube	1.35 m
6.	Height of sprayer above tube	30 mm
7.	Material	Al 6061 T6
8.	Effective heat transfer area	0.969 m <sup>2</sup>
9.	No of dummy tubes	6
10.	No of heated tubes	9
11.	Configuration of tube bundle	Inline and staggered
12.	Tube pitch	30 mm
13.	Heater rating/tube	3 kW

Table 2  
Specification of electric heating unit

Low-density cartridge heater	Make: digiquil systems Type: electric cartridge heater Diameter of the rod: 22 mm Length of the heating rod: 1,300 mm Input supply: 230 and 415 V Power: 3,000 W Operating temp: 250°C Material: stainless steel
Temperature controller	Make: digiquil systems PID controller: Size : 96 mm × 96 mm Control action: PID reverse action Input: thermocouple Output: relay output Alarm: 1° deviation high alarm Power: 85–265 VAC

#### 4. Experiment procedure

Heater and chiller are switched ON for maintaining the fixed temperature for the hot water and cold water storage tanks. Automatic cut-off is provided, once the temperature reaches the set value of temperature. Vacuum pump is operated to maintain the evaporator and condenser at the required vacuum conditions corresponding to the saturation temperature of the feed water. Feed water pump is switched ON and the required quantity of hot water is supplied to the evaporator through the spray systems. The water sprayed over the tube bundle is flowing down as thin film over the tubes. First two rows are dummy tubes and the last three rows of tubes are heated internally. Tube wall is assumed to be at constant temperature and maintained above the saturation temperature of vapor. The vapor generated from the evaporator is passed on to the condenser. Vapor stream also contains the non-condensable gases liberated from feed water by degassing under vacuum conditions. Un-evaporated liquid water is pumped back to the heater tank using a pump. The condenser is supplied with chilled water to condense the vapor entered into it and the distillate produced is collected at the bottom of the condenser. Vacuum pump is continuously operated to remove the non-condensable gases liberated. Experiments were conducted with varying parameters, such as feed flow rate, feed temperature, saturation pressure, thermal spray coated and uncoated tubes, inline and staggered configuration of tube bundle, etc. The plain tubes were tested first and spray-coated tubes of different coating thicknesses were tested later. The Scanning Electronic Microscope (SEM) view of the plain and coated surface is shown in Fig. 5.

Copper-Constantine thermocouple was used for temperature measurements with an uncertainty of  $\pm 0.1^\circ\text{C}$ . Vacuum transmitter with  $\pm 0.2\%$  accuracy was used to measure the vacuum in the evaporator. Glass

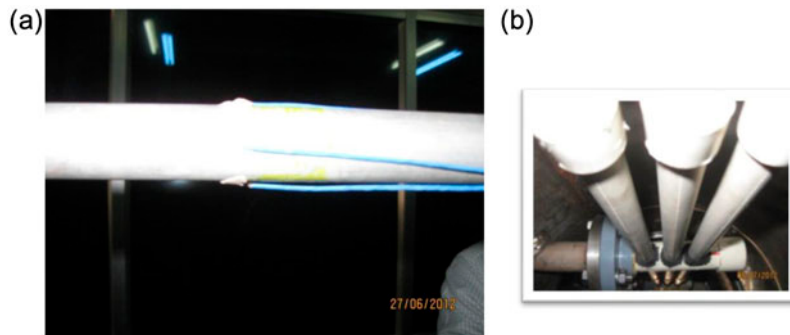


Fig. 4. (a) Typical location of thermocouples around the tube and (b) spray nozzle.



Rotameters were used to measure water flow rate in circuits with an uncertainty of  $\pm 2.0\%$ . All the instruments were calibrated before starting the experiments. Tables 3 and 4 provide the details of the instruments used with their range and accuracy. Measurements on mass flow rates, tube wall temperature, saturation temperature of vapor, inlet and outlet temperature of water, etc. have sensitive impact on the heat transfer coefficient. An error analysis was carried out for the measurement of heat load and heat transfer coefficient and it was found that results are within the error limits of  $\pm 2.24$  and  $\pm 5.8\%$ , respectively.

## 5. Results and discussion

The pressure and temperature conditions of the experimental system are typical operating conditions of a first-effect MED system. Normally, top brine temperature is limited to  $75^\circ\text{C}$  to prevent scaling on tubes. The falling film Reynolds number of desalination system ranges from 300 to 1,500. The feed flow rate in the experimental system was varied from 800 to 3,000 kg/h. This is equivalent to film Reynolds number 200–800. The active length of the nine heated tubes was used for heat transfer area calculations. Wall temperatures of the tubes were measured using thermocouples inserted on the tube wall. Four thermocouples were fixed on the circumference of the tube to measure the top, bottom and sidewall temperatures. The temperature of feed water was varied from  $55$  to  $75^\circ\text{C}$ . A computerized Data Acquisition System (DAS) was used for collecting and storing data (Table 5). Experiments were carried out with fresh water as well as sea water. Table 6 gives the difference in properties of fresh and sea water.

### 5.1. Temperature profile in the system

Fig. 6 shows a typical operating condition (average data) in the evaporator for the duration of one hour. Warm feed water is sprayed over the tube bundle at an average of temperature of  $68.7^\circ\text{C}$  while the evaporator tube wall temperature is maintained at about  $73.6^\circ\text{C}$ . The heated feed water leaves the evaporator at about  $71.4^\circ\text{C}$ . The saturation pressure and temperature in the evaporator is maintained as 332.36 mbar and  $71.4^\circ\text{C}$ , respectively. Heat transfer from the wall to vapor across the film is taking place at a temperature difference ( $\Delta T_e$ ) of  $2.2^\circ\text{C}$ .

Temperature around the wall is measured using four thermocouples fixed all around at  $90^\circ$  angle as shown in Fig. 4(a) corresponding to a cut-off wall temperature  $55^\circ\text{C}$  for the duration of one hour. The output temperature readings are plotted in Fig. 7. It was observed that highest temperature is at the bottom of the tube ( $180^\circ$  from top) indicating flow stagnation or dry out condition. Higher fluctuation of temperature at the bottom of the tube proves the local dry out or mal-distribution of flow at the bottom region of the tube surface. Similarly the top of the tube also shows higher temperature than the side wall of the tube indicating stagnant region. Fig. 8 shows the temperature profile around the tube for various Reynolds numbers. The reduction in temperature at  $90^\circ$  angle of the tube can be attributed to the thinning of film and increase in fluid velocity. The downward trend in temperature profile is different in the developing region at the top of the tube and this indicates the need of measurements in close range. Experimental studies of Parken et al. used measurements in a close range of  $45^\circ$ . However the temperature measurements were not reported.

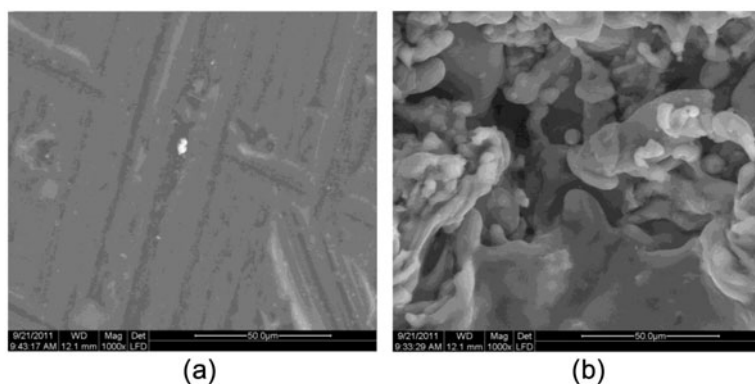


Fig. 5. SEM view (a) plain Al tube and (b) coated Al tube.

Table 3  
Range and accuracy of measurements

Quantity	Instrument	Make	Range	Accuracy (%)
1. Feed water flow rate	Glass rotameter	Instrumentation Engineers Pvt Ltd,	320–3,200 kg/h	±2.0
2. Reject water flow rate	Glass rotameter	India	320–3,200 kg/h	±2.0
3. Cooling water flow rate	Glass rotameter		320–3,200 kg/h	±2.0
4. Temperature	Cu-Constantine thermocouple		–200 to 350°C	±0.1
5. Vacuum	Vacuum transmitter	Yokogawa	0–1.05 bar	±0.2
6. Digital data	DAS system	Agilent	0–250 channels/s	±0.004

Table 4  
Specification of vacuum transmitter and rotameter

	Vacuum transmitter	Rotameter
Make	Yokogawa	Instrumentation engineers
Temperature	0–100°C	57.5°C AVG
Range	0–1 kgf/cm <sup>2</sup>	320–3,200 L.P.H.
Input	8–30 V DC	Down
Output	4–20 mA	Up
Type	Piezoresistive	Vertical float
End connection	¼" male NPT	1" Screwed N.P.T(F)
Fluid	Steam/water	Water
Material	Stainless steel	Stainless steel 316
Accuracy	±0.2%	±2.00% FSD

### 5.2. Effect of film Reynolds number on heat transfer

Feed flow rate of water to the evaporator is influencing the heat transfer characteristics, such as film thickness, film coefficient, the mode of the flow between tubes, etc. Film Reynolds number was increased from 200 to 800 which are within the normal operating range of thermal desalination systems. The influence on distillate generation is studied as shown in Fig. 9. Experiments were conducted at three different wall temperatures such as 58, 65, and 75°C. The increase in generation of distillate with increase in temperature can be noticed, but there is an optimum film value of  $Re = 400$  approximately at which it is maximum. This indicates that though the local film coefficient is increased with feed rate due to higher fluid velocity, increase in film thickness reduces the overall heat transfer and evaporation.

Influence of film Reynolds number of heat transfer coefficient is plotted in Fig. 10. Bundle average heat

transfer coefficient for varying film Reynolds number is plotted for fresh water as well as for sea water. The details of the tube bundle configuration are given in Table 1. Experimental results of Parken et al. reported variation of local heat transfer coefficient from 4,500 to 6,500 W/m<sup>2</sup> K for distilled water feed rate of 0.135–0.284 kg/ms ( $Re = 1,020$ – $2,150$ ). Increasing the feed water temperature from 45 to 100°C has resulted about 20% increase in film coefficient. Inline and staggered tube configuration is compared and it is observed that inline configuration gives a better film coefficient. This can be due to more stabilized flow and tube wetting in falling film for inline configuration compared to staggered configuration. The tests are repeated with sea water and fresh water. The optimum conditions under vacuum for a temperature range of 55–75°C for heat transfer coefficient (6,500–6,800 W/m<sup>2</sup> K for fresh water) are obtained during the range of film Reynolds number 400–600. Results of Computational Fluid Dynamic (CFD)

Table 5  
Specification of DAS

Data acquisition unit and accessories	ElmackEngg Services, India Make: Agilent <b>34970A (data acquisition/switch unit):</b>
	<ul style="list-style-type: none"> <li>• <math>6\frac{1}{2}</math> digit multimeter accuracy, stability, and noise rejection. Up to 60 channels per instrument</li> <li>• Reading rate is 600 reading per second on single channel</li> <li>• Scan rate is 250 channels per second</li> <li>• GPIB (IEEE-488) interface and RS-232 interface standard</li> <li>• SCPI compatibility</li> <li>• Direct measurement of Thermocouples, AC/DC current, RTD, thermistors, AC/DC voltages, etc.</li> </ul>
	<b>34901A (20 channel armature multiplexer):</b>
	<ul style="list-style-type: none"> <li>• 20 Channel of 300 V switching</li> <li>• Two channel for DC/AC current measurement (100 mA–1 A)</li> <li>• Switching speed of up to 60 channels per second</li> </ul>

Table 6  
Properties of water and sea water

	Water at 60°C	Sea water at 60°C (40 ppt)
Density, kg/m <sup>3</sup>	983.3	1012.7
Dynamic viscosity, kg/m s	0.000476	0.000716
Surface tension, N m	0.06624	0.0675
Specific heat, J/kg K	4,185	3,983
Conductivity, W/m K	0.652	0.649

studies on sea water with a bundle of five inline and staggered tubes also shown for comparison. A recent study by Mu et al. [14] on 25.4 mm Al-brass tubes under vacuum conditions reported that heat transfer coefficient gradually increases from 4,000 to 7000 W/m<sup>2</sup> K for a feed rate of 0.02–0.07 kg/ms ( $Re = 150$ – $520$ ) and a declining trend beyond. Feed water temperature was varied from 45 to 70°C. Studies with sea water showed a reduction of 15–20% in film heat transfer coefficient.

### 5.3. Mass of evaporation

Effect on mass evaporation of feed water at three different temperatures such as 58, 65, and 75°C are shown in Fig. 11. The higher evaporation rate is observed at higher temperature due to reduction in viscosity, density, surface tension, etc. Increase in surface heat transfer coefficient with feed water inlet temperature was reported by Parken et al. and Mu et al. in their experimental studies. However, the evaporation occurs at liquid–vapor interface and behaves differently with feed rate or film Reynolds number. CFD studies on evaporation on 19.04, 25.4, and 50.8 mm tube sizes were carried out and compared with experimental results. More details of the CFD studies on falling film evaporation were discussed by Abraham and Mani. The optimum film evaporation conditions are obtained at  $Re = 700$ – $800$  as per CFD predictions. However, experimental studies show that the optimum

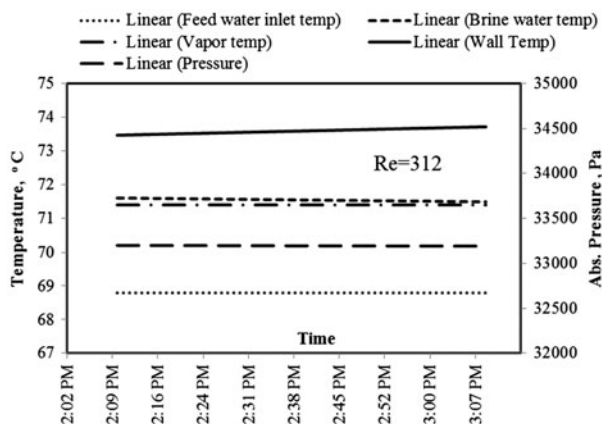


Fig. 6. Operating conditions in the evaporator for  $Re = 312$ .



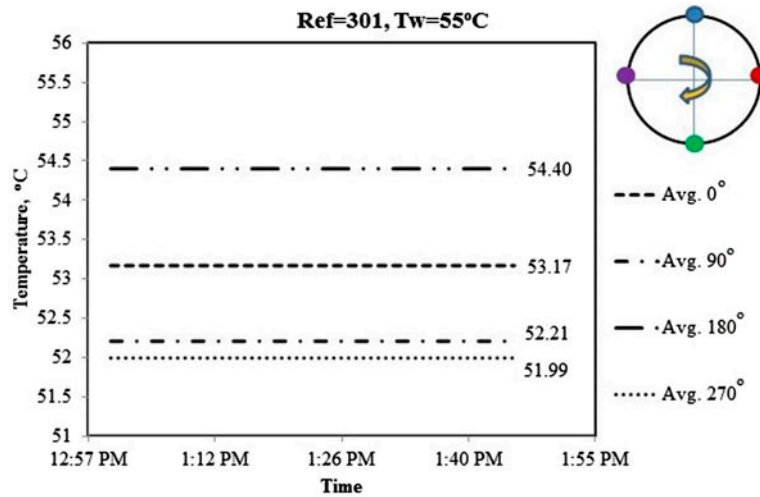


Fig. 7. Measured temperatures around tube wall for  $Re = 301$ .

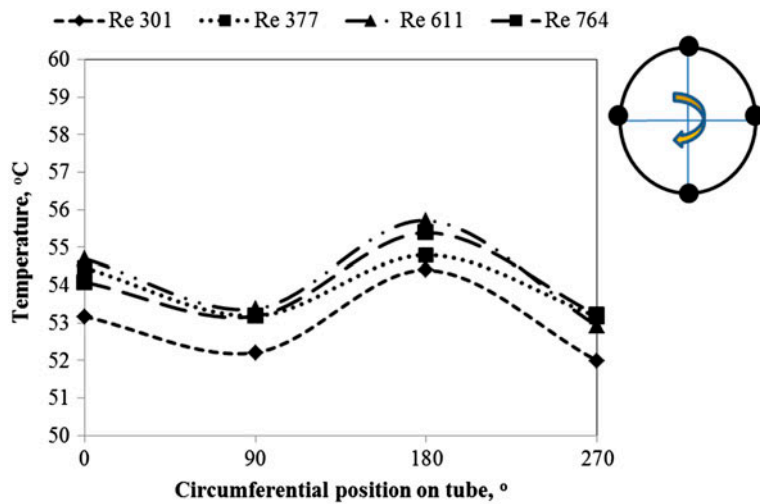


Fig. 8. Experimental temperature profile around tube wall varying Reynolds numbers.

results are at  $Re = 400\text{--}500$ . The difference can be due to the uncertainties involved in the experimental studies especially due to non-uniform temperature on the wall surface. The result of the experimental studies reported by Sharma and Mitra [15] is also plotted and the optimum evaporation observed at a film Reynolds number of 600–700. This was based on a study carried out with brackish water for aero–evapo–condensation process at atmospheric conditions. Feed water was supplied to the bundle of tubes at 50°C. Splashing of water was reported at higher Reynolds numbers causing reduction in evaporation in experimental studies. More accurate data can be obtained when the electric

heaters are replaced with condensing steam in the present experimental setup.

#### 5.4. Influence of thermal spray coating

Heat transfer enhancement with the porous surface by thermal spray coating is due to the complete solution wetting and increased thin film evaporation from the menisci in the porous matrix. In order to study the effects of thermal spray coating on heat transfer enhancement, experimental studies were carried out with bare Aluminum tubes and coated tubes. Molten Aluminum was sprayed over the cylindrical Aluminum

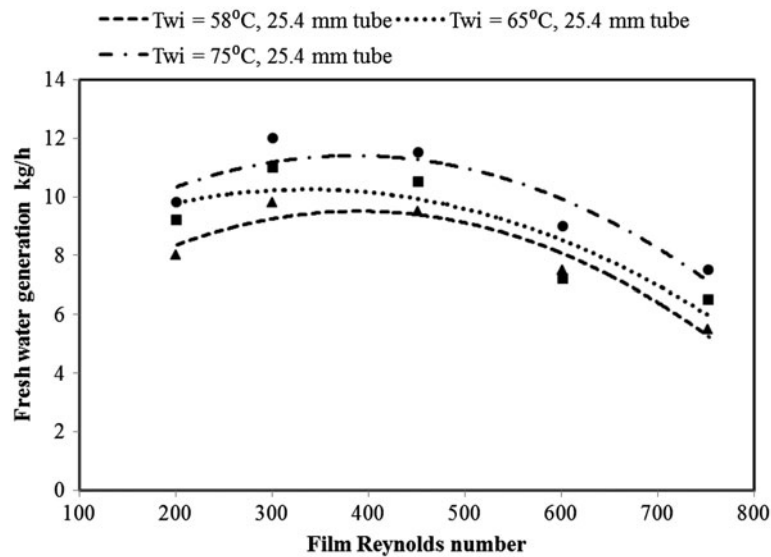


Fig. 9. Distillate generation on inline tube bundle of 25.4 mm Ø plain tubes.

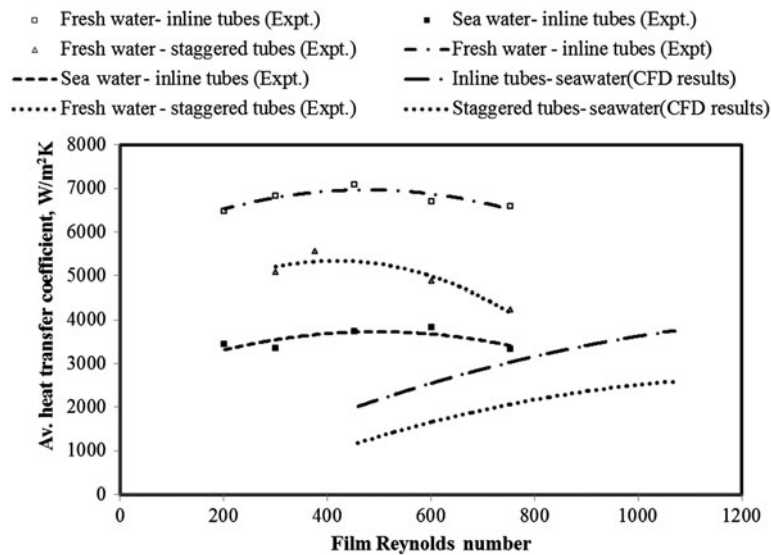


Fig. 10. Comparison of CFD and experimental heat transfer coefficient.

tubes using flame spray technology. Tubes with various coating thickness ranging from about 0.4 to 1.0 mm and porosity 15–20% were tested. The experimental results are shown in Fig. 12. Falling film evaporation is enhanced mainly by the increase in turbulence level and reduction in film thickness in a thermal spray coated surface. No nucleate boiling was observed as the wall super heat is limited to about 2.5°C. Higher enhancement can be expected with increase in wall heat flux due to nucleate boiling. Similar enhancement of distillate production was observed for tests with sea water condition. The increased production of distilled

water with thermal spray-coated tubes is 75–150% higher than that of uncoated tubes. Tests were conducted for two months duration and longer duration testes are recommended for understanding the effects of scaling or fouling. Experimental studies of Bogan and Park [16] on porous coating of copper particles on copper tube of 15.88 mm with 0.8 mm coating thickness, reported about 20% enhancement in heat transfer for distilled water under sub-cooled conditions for a range of Reynolds number from 120 to 380. The presence of porous coating enhances the heat transfer due to the increased turbulence level and the possibility of

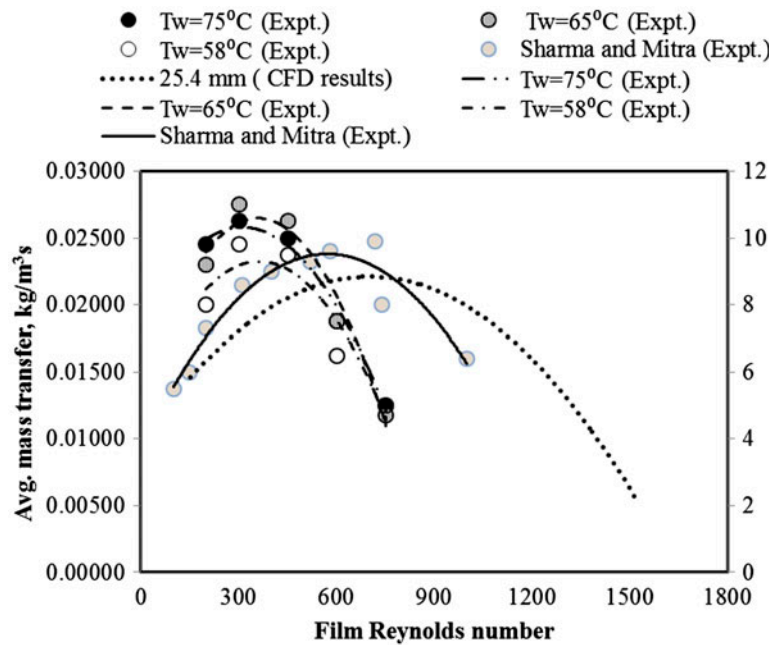


Fig. 11. Experimental results of mass transfer at different temperatures.

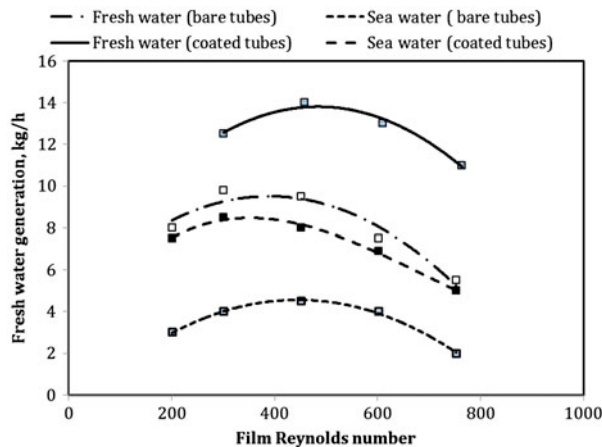


Fig. 12. Distillate generation for bare and thermal spray-coated tubes.

nucleation at higher heat flux conditions. Mass transfer of liquid film is improved due to the reduction in film thickness with film waviness and enhancement in heat transfer rate. Further investigations on the coupling of these two phenomena are required.

### 6. Conclusions

Experimental studies were carried out for horizontal tube falling film evaporation with 25.4 mm Al tube bundle of 3 × 5 configurations for a range of Reynolds numbers between 200–800 with fresh water and sea

water. The tube wall temperature is observed to be highest at bottom and top of the tube indicating flow stagnation or detachment at the bottom of the tube. The optimum Reynolds number for the best distillate production is around  $Re = 400$ . This was compared with the data available in the literature and CFD studies. Plain and thermal spray-coated tubes were tested and experimental studies show about 75–150% improvements in performance with thermal spray-coated tubes. However, long-term operational data is to be established for estimating the effects of scaling on the tube surfaces.

### Acknowledgment

Authors acknowledge the financial support received from National Institute of Ocean Technology, Chennai.

### Nomenclature

$A$	— heat transfer area, $m^{-2}$
$C_p$	— specific heat, $J\ kg^{-1}\ K^{-1}$
$d_o$	— tube outside diameter, m
$g$	— gravitational acceleration, $ms^{-2}$
$Ga$	— Galileo number, $gl^3\rho^2\mu^{-2}$
$h$	— heat transfer coefficient, $Wm^{-2}\ K^{-1}$
$h_{fg}$	— latent heat of vaporization, $kJ\ kg^{-1}$
$k$	— thermal conductivity, $Wm^{-1}\ K^{-1}$
$L$	— effective tube length, m
$Nu$	— Nusselt number, $h\nu^{2/3}k^{-1}g^{-1/3}$
$Pr$	— Prandtl number, $\mu C_p k^{-1}$
$q$	— heat flux, $W/m^2$

$r$	— outer tube radius, m
$Re$	— film Reynolds number, $4\Gamma\mu^{-1}$
$s$	— tube pitch, m
$\Delta T_e$	— local temperature difference for evaporation, K
HTC	— heat transfer coefficient, $Wm^{-1}K^{-1}$

#### Greek symbols

$\Gamma$	— half liquid mass flow rate per unit length of tube, $kg\ m^{-1}s^{-1}$
$\delta$	— film thickness, mm
$\theta$	— angle along the tube perimeter measured from the apex,
$\mu$	— dynamic viscosity, $kg\ m^{-1}s^{-1}$

#### Subscripts

$e$	— evaporation
$f$	— fluid
$i$	— inlet
$l$	— liquid
$s$	— saturated
$o$	— outside
$w$	— wall

#### References

- [1] L.S. Fletcher, V. Sernas, W.H. Parken, Evaporation heat transfer coefficients for thin sea water films on horizontal tubes, *Ind. Eng. Chem. Process Des. Dev.* 14(4) (1975) 411–416.
- [2] W.H. Parken, L.S. Fletcher, V. Sernas, J.C. Han, Heat transfer through falling film evaporation and boiling on horizontal tubes, *J. Heat Transfer* 112 (1990) 744–750.
- [3] P.K. Tewari, R.K. Verma, M.P.S. Ramani, A. Chatterjee, S.P. Mahajan, Nucleate boiling in a thin film on a horizontal tube at atmospheric and subatmospheric pressures, *Int. J. Heat Mass Transfer* 32(4) (1989) 723–728.
- [4] X. Hu, A.M. Jacobi, The inter tube falling film: Part 1 —Flow characteristics, mode transitions, and hysteresis, *J. Heat Transfer* 118(3) (1996) 616–625.
- [5] L. Yang, S. Shen, Experimental study of falling film evaporation heat transfer outside horizontal tubes, *Desalination* 220(1–3) (2008) 654–660.
- [6] H. Hou, Q. Bi, H. Ma, G. Wu. Distribution characteristics of falling film thickness around a horizontal tube, *Desalination* 285 (2012) 393–398.
- [7] M.C. Chyu, A.E. Bergles, Horizontal-tube falling-film evaporation with structured surfaces, *J. Heat Transfer* 111 (1989) 518–524.
- [8] M.S. Alam, L. Prasad, S.C. Gupta, V.K. Agarwal, Enhanced boiling of saturated water on copper coated heating tubes, *Chem. Eng. Process.* 47(1) (2008) 159–167.
- [9] V.J. Lakhera, A. Gupta, R. Kumar, Investigation of coated tubes in cross-flow boiling, *Int. J. Heat Mass Transfer* 52(3–4) (2009) 908–920.
- [10] W. Li, X.Y. Wu, Z. Luo, R.L. Webb, Falling water film evaporation on newly-designed enhanced tube bundles, *Int. J. Heat Mass Transfer* 54(13–14) (2011) 2990–2997.
- [11] R. Abraham, A. Mani, Effect of flame spray coating on falling film evaporation for multi-effect distillation system, *Desalin. Water Treat.* 51(4–6) (2013) 822–829.
- [12] G. Ribatski, A.M. Jacobi, Falling-film evaporation on horizontal tubes—A critical review, *Int. J. Refrig.* 28 (2005) 635–653.
- [13] M.C. Chyu, A.E. Bergles, An analytical and experimental study of falling-film evaporation on a horizontal tube, *J. Heat Transfer* 109(4) (1987) 983–990.
- [14] X. Mu, S. Shen, Y. Yang, X. Liu, Experimental study of falling film evaporation heat transfer coefficient on horizontal tube, *Desalin. Water Treat.* 50(1–3) (2012) 310–316.
- [15] R. Sharma, S.K. Mitra, Performance model for a horizontal tube falling film evaporator, *Int. J. Green Energy* 2 (2005) 109–127.
- [16] N. Bogan, C. Park, Influences of solution sub cooling, wall superheat and porous-layer coating on heat transfer in a horizontal-tube, falling-film heat exchanger, *Int. J. Heat Mass Transfer* 68 (2014) 141–150.